Chapter 6
Structural Channels as Natural Tracks in Crystal

D. Fuks, A.E. Kiv, and D. Fink

Abstract It has been shown that filling the parallel structural channels in crystals with metal ions may lead in some cases to the creation of new electronic materials with metallic nanowires in a solid matrix. It is expected that such material should exhibit effects similar to the earlier developed "TEMPOS" structures (which are electronic devices that consist of metal nanoparticle-filled etched tracks in oxide layers on Si substrates) however, greatly reduced in scale. These structures are, therefore, considered as useful additions to nano-electronics. Density Functional Theory (DFT) is applied to demonstrate that Li nanowires can be incorporated into structural channels of $Ni_{12}P_5$ crystal under thermodynamic conditions of crystal growth. Ab initio calculations of electronic states in the system $Ni_{12}P_5$ + Li have been carried out.

D. Fuks
Department of Materials Engineering, Ben-Gurion University of the Negev,
PO Box 653, Beer-Sheva 84105, Israel
e-mail: fuks@bgu.ac.il

A.E. Kiv (✉)
Department of Materials Engineering, Ben-Gurion University of the Negev,
PO Box 653, Beer-Sheva 84105, Israel

Department of Physical and Mathematical Modelling, South-Ukrainian National Pedagogical University, 26 Staroportofrankovskaya, 26020 Odessa, Ukraine
e-mail: kiv@bgu.ac.il

D. Fink
Instituto de Fisica, Universidade Federal do Rio Grande do Sul, Campus do Vale,
91501-970 Porto Alegre, RS, Brazil

Departamento de Fisica, Universidad Autónoma Metropolitana-Iztapalapa,
PO Box 55-534, 09340 México, DF, Mexico

Nuclear Physics Institute, 25068 Řež, Czech Republic

Berlin Helmholtz-Zentrum fuer Materialien und Energie, Lise-Meitner Campus,
Glienicker Str. 100, 14109 Berlin, Germany
e-mail: fink@xanum.uam.mx; fink@daad-alumni.de

Y.N. Shunin and A.E. Kiv (eds.), *Nanodevices and Nanomaterials for Ecological Security*, NATO Science for Peace and Security Series B: Physics and Biophysics, DOI 10.1007/978-94-007-4119-5_6,

Keywords Ion tracks electronics • Ions channeling in crystals • DFT calculations • $Ni_{12}P_5$ + Li system

6.1 Introduction

6.1.1 Ion Tracks in Non-metallic Materials

Besides the conventional semiconductor electronics and molecular electronics, nowadays there is also another alternative field, the so-called "ion track electronics" that attracts an increasing interest, especially for biosensing. The swift heavy ion irradiation of insulating layers leaves behind them the "latent" ion tracks, which can be filled with various (semi)conducting materials (either in the shape of compact nanowires or nanotubules or dispersed nanoparticles) after etching them to the desired size and shape. Thus, electronic devices with a multitude of embedded parallel (conducting or semiconducting) pathways can be created that are absent in the classical field effect transistor concept.

Following this approach, novel multifunctional electronic devices with unique parameters (such as oscillators, amplifiers, tunable flip-flops, sensors, and diodes, logic AND/OR switches, artificial neural networks etc.) have already been created that were hitherto unknown in electronics [1–15]. One of these device families are TEMPOS structures (***T***unable ***E***lectronic ***M***aterial in ***P***ores in ***O***xide on ***S***emiconductors), see as an example the principal sketch in Fig. 6.1.

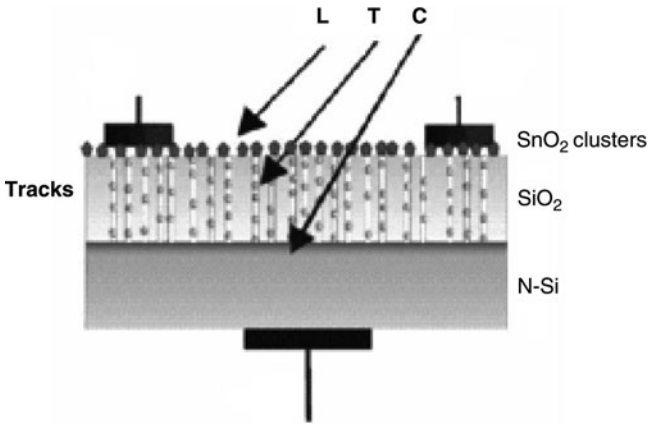

Fig. 6.1 Principle sketch of a TEMPOS element (shown here with oxide nanoclusters in the tracks and on surface). *L* surface layer, *T* (semi)conducting pores (such as *filled etched tracks*), *C* conducting silicon channel [16] shown here for the example of SnO_2 clusters as semiconducting surface deposition and pore fillings. The SnO_2 can be functionalized by attached organic functional groups

In contrast to the classical electronics all contacts are connected here conductively as well as capacitively to the device.

The incorporation of suitable materials in the etched tracks [8] and on the surface of TEMPOS structures transforms the latter ones, for example, to sensors for physical, chemical or biological signals. Sensing properties for many physical and chemical parameters such as light, temperature, magnetic fields, humidity and ammonia vapor have already been proven [1–6].

The independence of nanowires from each other which allows one to design intelligent track-to-track interaction strategies leads, among other unusual properties, to the emergence of negative differential resistances (NDR). A basic precondition for the occurrence of the NDR is that different ion track diodes (i.e., the ion tracks that are rectifying due to, e.g. the semiconductor-metal Schottky transition between the silicon substrate and metallic nanoparticles embedded in the tracks) of the TEMPOS structures operate at different working points (due to their individual track surface potentials mediated by the different potentials applied to the two surface electrodes). This condition implies non-zero inter-track currents, which, upon suitable applied external potentials, may lead to a collective abrupt inversion of the working points of all track diodes from closed to open (or vice versa), with a concomitant transient release of internally stored charges that shows up as NDR.

Another important direction of track electronics is based on electrolytes in etched tracks (***E***lectronics with ***E***lectrolytes in ***E***tched ***T***racks, E^3T) [17–22]. It has been demonstrated that fundamental electronic elements such as resistors, capacitors, diodes, sensors, pulse generators and elements with NDR can be produced in this way. As these structures are quite biomimicking they appear especially suitable for biotechnological tasks.

It is known that individual electrolyte-filled narrow pores such as etched ion tracks in thin polymeric films exhibit two different working states, a high-Ohmic and a low-Ohmic state, between which random and irregular jumps may occur [17]. Recently, we have recorded much more regular pulsations (repeating pulse parcels or current oscillations) in both latent and etched tracks [21], by making additional use of the effect of collective synchronization of random current spikes emitted from individual electrolyte-filled tracks. Both E^3T and E^3T/TEMPOS hybrids appear useful for biomedical applications, see e.g [18–20].

6.1.2 Channelling of Fast Particles in Crystals

The effect of fast ion channeling in crystals was discovered and explained more than 40 years ago [23, 24]. Because of the symmetrical arrangement of lattice atoms in a monocrystal, fast ions can penetrate deeper along the major crystal axes (e. g. (110), (111), (100) in the diamond-like lattice) and planes than in a random direction. Within these channels the ions stopping occurs only electronically, and the ion penetration distance is proportional to their velocity. This phenomenon is

Table 6.1 Critical angles (in degrees) for Boron ions in Si for three crystallographic directions

Energy (keV)	(100)	(110)	(111)
10	4.76	6.97	5.30
100	2.67	3.47	2.98
300	2.03	2.98	2.26

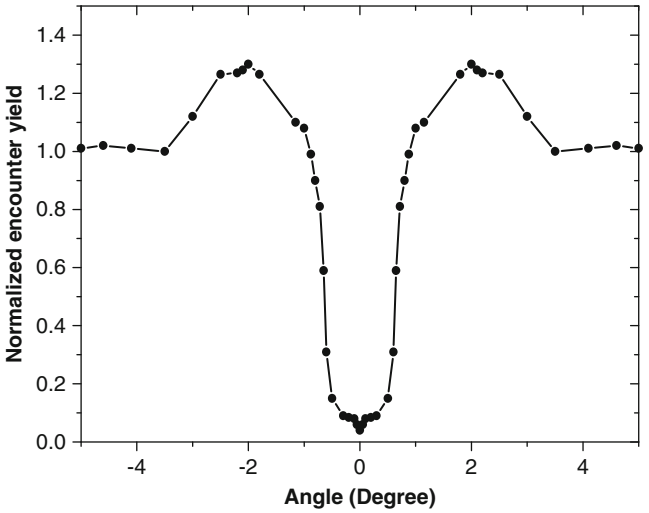

Fig. 6.2 Axial channelling dip for 3 MeV protons along (110) direction in Silicon [26]

called channeling and it finds a widespread application in the field of crystallography, ion implantation, in the investigations devoted to determination of the lattice location of impurity atoms and defects.

In the classical theory of channeling, the trajectory of ions is determined by the effective potential well with the minimum at the channel axes. The theory allows finding the critical angle (in degrees), below which an ion can enter into a channel without leaving it again [25]:

$$\phi_c = (Z_1 Z_2 a_0 E_R / dE)^{1/2}, \tag{6.1}$$

where Z_1 and Z_2 are the effective charges of the fast ion and the ions of the host lattice respectively, $a_0 = 0.53$ Å is the Bohr radius, $E_R = 13, 6$ eV is the Rydberg energy, d is an interatomic distance, and E is the energy of the incident ion.

In Table 6.1 [25] the critical angles for channeling of Boron in Silicon are presented for illustration.

The dependence of the channeling effect on the orientation of crystal with respect to the direction of ion beam for protons penetration into silicon is shown in Fig. 6.2 [26]. As follows from (6.1), the critical angle in the channeling effect decreases when the energy of ions increases. Theoretical studies and experimental measurements show that in typical cases the critical angle is $\pm 5^\circ$ in the energy

region ~10 keV and is ±1° when the energy is ~1 MeV [25]. All the presented considerations are valid for heavy charge particles, but not for electrons or positrons. In the last case the diffraction and tunneling effects would influence significantly the channeling of particles in crystals. Investigations of the channeling effect in crystals have led to obtaining information regarding the nature of interatomic interactions and parameters of interatomic potentials in the region of structural channels of crystals [24, 25]. Although these parameters depend on the energy interval, they can be useful for determining interatomic potentials in equilibrium conditions.

Structural channels have to be taken into account while dealing with the problem of ion implantation aimed to modify materials and to produce electronic devices. In many cases the penetration of ions into channels changes the concentration profile for implanted ions when this profile has to be sharp. But in other cases it would be desirable to fill the structural channels by a corresponding substance in order to get a solid matrix with parallel nanowires in channels. Further we show that such possibility can appear for some crystals in the process of thermodynamic crystal growth.

6.2 Metallic Nanowires in Crystal Channels (Li in $Ni_{12}P_5$)

As mentioned above, the channels in crystals form one-dimensional (1D) potential wells that provide favorable conditions for a long-range penetration of fast ions into crystals. Due to the symmetric arrangement of lattice atoms in the channel, the minimum of potential well is located geometrically in the centre of the channel. Within these channels the energy loss by the fast ion is determined only by the ion-electron interactions. There are practically no nuclear collisions.

Proceeding from these considerations, we suggest that the crystal channels inherent for some crystallographic structures can be used to create quasi-one-dimensional conducting chains of metallic atoms inside them. One of the examples of such a crystallographic structure is $Ni_{12}P_5$ (Space Group *I4/m* (87)). In Table 6.2 the Wyckoff positions of Ni and P atoms are presented. Other compounds with the same structure are $Co_2Ni_{10}P_5$ and $Pt_{12}Si_5$.

This crystallographic structure contains channels normal to (001) plane in the tetragonal cell. The results of 1D crystal growth within single walled carbon nanotubes (SWNTs) [27] present an interesting analog in this context. As SWNTs form atomically thin channels within a restricted diameter range, their internal

Table 6.2 Structure of Ni12P5 compound (sites of atoms or atomic structure)

Atom	Site	x	y	z
P(1)	2a	0	0	0
Ni(1)	8h	0.3655	0.0609	0
Ni(2)	16i	0.1166	0.1812	0.2490
P(2)	8h	0.1939	0.4132	0

van der Waals forces regulate the growth behaviour of encapsulated materials in a precise fashion. In [27, 28] it has been found that the crystal growth within SWNTs is atomically regulated, and nano-scale crystals with precise architectures can be formed.

Crystals with metallic chains (nanowires) embedded in their structural channels can be considered as electronic structures similar to those described in Sect. 6.1. Whereas in all previous structures, some 10^6–10^9 (semi)conducting tracks interacted/ with each other in test samples of 1 cm^2 area (thus resulting in about 0.5–10 μm average track-to-track distance), the inter-channel distance in the new crystal-channel structures, CCS is ∼0.5 nm, i.e. about 10^3–10^4 times shorter. Hence, the expected nanowire density in CCS will be ∼10^6–10^8 times larger than in the corresponding TEMPOS structures, thus leading to truly nanometric electronic materials with greatly enhanced possibilities. It is assumed that scaling down both the average nanowire distances and the distances between the external electrical contacts from TEMPOS or E^3T structures to CCS by the same factor should leave their electronic device properties largely unchanged. Applying such a scaling law, a square CCS of only (0.5–10) μm × (0.5–10) μm size would correspond to the hitherto used 1 cm × 1 cm large TEMPOS, or E^3T test structures.

Of course, the possibilities to vary electronic parameters in CCS are somewhat more limited in comparison with the structures of the previously developed larger-scale track electronics. However, one can expect that the basic effects of track electronics will be preserved by this scaling-down approach, and possibly even new features will be opened in CCS – essentially due to the much higher available nanowire density in CCS – so that CCS will become a very useful add-on to track electronics.

To analyze the problem, we have chosen $Ni_{12}P_5$ and Li atoms, to study the possible formation of Li nanowires in $Ni_{12}P_5$ channels. The Density Functional Theory (DFT) has been applied [29–35], and the mixing energy for the $Ni_{12}P_5$ + Li system has been calculated as well as the spatial distribution of differential electron density (DED) and the Density of States (DOS) for the system. The software package WIEN2k-09.2 [36] was used for the electronic structure calculations.

We performed the investigation of the electronic structure of $Ni_{12}P_5$ to confirm the preferable location of Li atoms in structural channels of this crystal and the formation of Li nanowires.

In Fig. 6.3 the nanochannels in $Ni_{12}P_5$ crystal (in (001) direction) are shown together with the incorporated Li atoms.

First, the preferable positions of Li atoms in the channels in $Ni_{12}P_5$ lattice have been determined. The total energy calculations have proved that Li atoms occupy the centre of a structural channel position in each cell and the distance between the minimal positions of the nearest potential wells is 0.5 a (a = 5.08 Å is the lattice parameter). Simple geometrical consideration shows that the inter-channel diffusion of Li atoms is practically impossible due to extremely high energy barriers along the corresponding diffusion paths. Thus Li atoms which in the statistical process of crystal growth appear in the given channel will further remain there in a stable state.

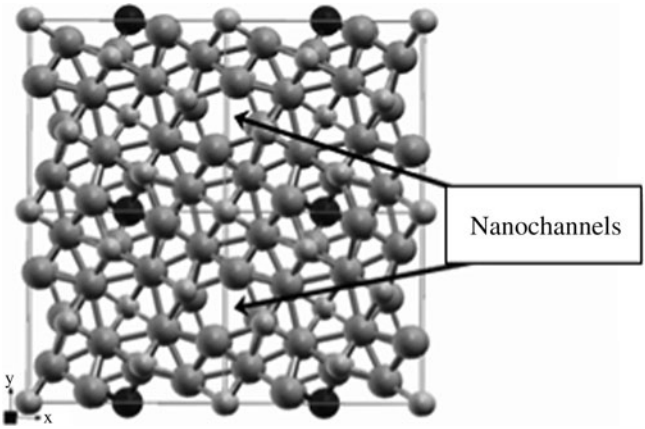

Fig. 6.3 Nanochannels in $Ni_{12}P_5$ crystal: Phosphorus atoms (*small grey balls*), Nickel (*large grey balls*) and Lithium (*black balls*)

To check the thermodynamic stability of $Ni_{12}P_5$ + Li system, the mixing energies (E_{mix}) for different atomic fractions, c, of Li in the channels have been calculated using the standard expression:

$$E_{mix}^{cell} = E_{Ni_{12}P_5+Li}^{cell} - \left(E_{Ni_{12}P_5}^{cell} + c \cdot E_{Li}\right), \tag{6.2}$$

where c is the fraction of the channel sites in the cell occupied by Li atoms. The mixing energies in all cases are negative.

The spatial distribution of DED has been calculated to analyze the redistribution of electrons in vicinity of Li atoms. The electron map in Fig. 6.4 displays the electron density in the plane containing one Li atom in the unit cell (x–z plane). The situation presented in Fig. 6.4 corresponds to the uniform arrangement of Li atoms along the channel with interatomic distance equal to the lattice parameter a. The concentration of Li atoms in $Ni_{12}P_5$ + Li system in this case is ∼0. 03. In Fig. 6.5 the charge distribution that corresponds to the concentration of Li atoms in the system ∼0.11 is presented. Here all possible occupation sites for Li atoms along the channel are filled with Li.

In the first case, the increase of the electron density between Li and Ni is observed, and the electron cloud is shifted to Ni atoms due to their larger electronegativity. This leads to significant heterogeneity of charge distribution along the channel. When the side-by-side location of Li atoms occurs along the channel, the increase of the electron density is observed *along* the channel, making it much more uniform (see Fig. 6.5).

At the same time, it is difficult to expect the possibility of charge transfer under the external voltage applied in the direction orthogonal to Li nanowires. As illustrated in Fig. 6.5, this direction is characterized by significant decrease of the electron density. The obtained result demonstrates that a set of parallel Li

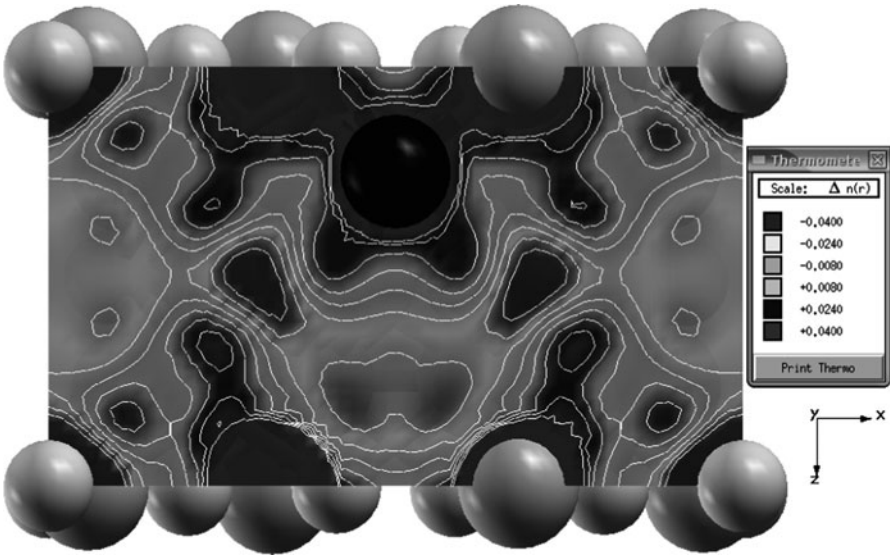

Fig. 6.4 DED in the $Ni_{12}P_5$ crystal with one Li atom in the unit cell

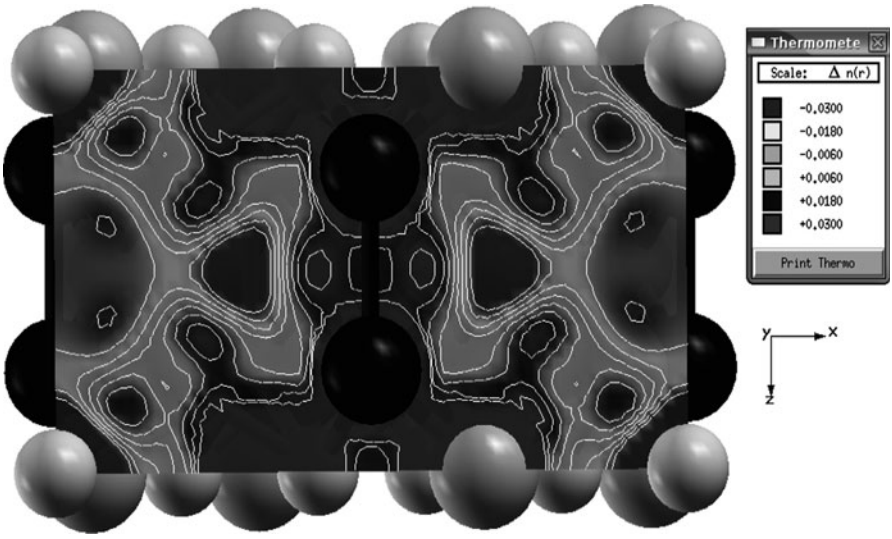

Fig. 6.5 DED in the $Ni_{12}P_5$ crystal with four Li atoms in the unit cell

nanowires with rather uniform axial electron charge distribution can be formed in such matrix. It is clear that in a real statistical process of crystal growth, we will get neither the first nor the second situation. Different channels will be filled by Li atoms in different ways. The occupation of each channel will be not uniform which

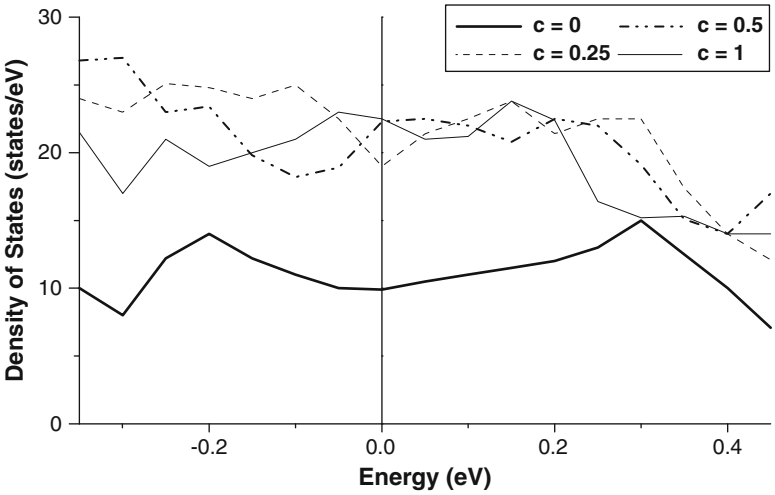

Fig. 6.6 DOS in the vicinity of Fermi level for $Ni_{12}P_5$ crystal with different atomic fractions of Li. Here and in following figures Fermi level is set to zero energy

prescribes them peculiar individualities. We can conclude that such a system of nanowires will have percolation conductivity. Moreover we foresee that it will be a percolation system with lateral dead tips. One can get the desirable characteristics of $Ni_{12}P_5$ + Li system by varying the technological conditions of crystal growth and the concentration of Li atoms. Apparently it is possible to create quite uniform Li nanowires in $Ni_{12}P_5$ crystals. The $Ni_{12}P_5$ + Li system demands further studies to deeper understand the nature of its electric conductivity and the ways of its modification for practical applications.

In this study we have obtained additional information regarding the chemical features and the electronic structure of $Ni_{12}P_5$ crystal with Li nanowires from calculations of DOS. We have observed how the incorporation of Li nanowires into $Ni_{12}P_5$ crystal changes the electronic states of the whole crystal and of its components, Ni and P. In Figs. 6.6, 6.7, and 6.8 DOS in the vicinity of the Fermi level are displayed. The notations in these Figures are given in terms of the numbers of Li atoms that occupy the channel sites in the unit cell. The maximal number of Li atoms in the unit cell is 4. Insertions in the Figures show three cases: only one Li atom is present in the unit cell (0.25), two atoms (0.5) and all four atoms are present in the unit cell (1). These three cases correspond to concentrations of Li atoms in the $Ni_{12}P_5$ + Li crystal, $C = 0.03$, 0.06 and 0.11, respectively. For comparison, the results for $Ni_{12}P_5$ structure without Li atoms are also presented.

Figure 6.6 shows that the smallest of the considered concentrations of Li atoms influences considerably the chemical bonding in $Ni_{12}P_5$ crystal. Indeed, the value of total DOS at the Fermi level increases approximately twice, and the dependence of this value on the concentration of Li atoms is weak in the considered C interval. Considering the obtained data it is possible to conclude that a new structure

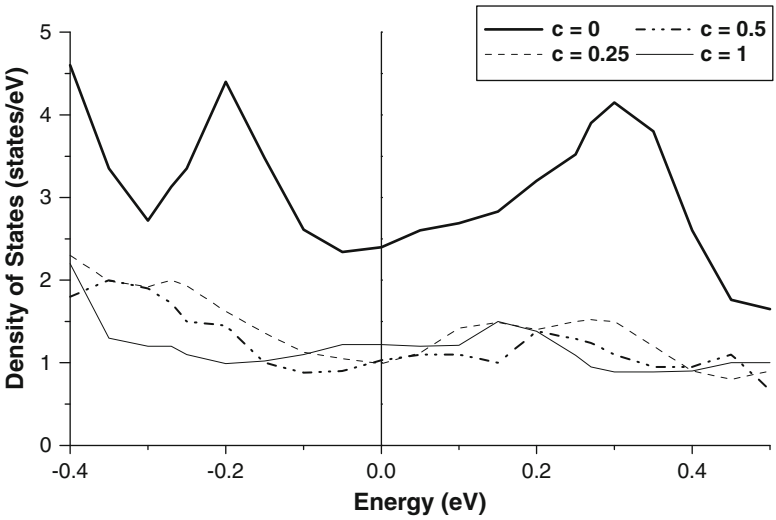

Fig. 6.7 Local DOS in the vicinity of Fermi level for Ni atom in $Ni_{12}P_5$ with different atomic fractions of Li

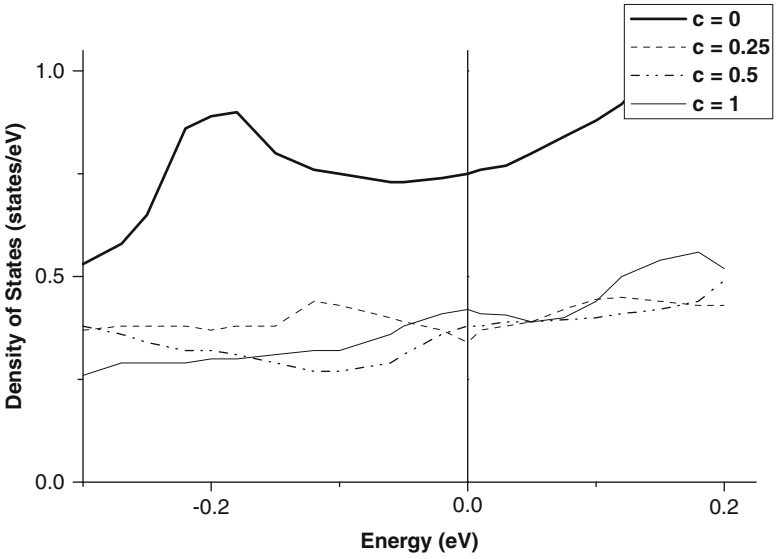

Fig. 6.8 Local DOS in the vicinity of Fermi level for P atom in $Ni_{12}P_5$ with different atomic fractions of Li

$Ni_{12}P_5$ + Li is not simply a $Ni_{12}P_5$ crystal doped by Li atoms. Instead, this is a significantly modified $Ni_{12}P_5$ crystal (CCS) with Li nanowires in structural channels.

Figures 6.7 and 6.8 show the influence of Li atoms on the local DOS for the closest to them Ni (Fig. 6.7) and P (Fig. 6.8) atoms in the $Ni_{12}P_5$.

One can see that an incorporation of Li atoms changes the electronic states in both cases almost identically. The detailed study of electronic transformations in CCS $Ni_{12}P_5$ + Li is important in order to understand the features of the conductivity of Li nanowires and the ways of application of such systems.

6.3 Discussion

Though quite a number of studies have been already performed on TEMPOS, E^3T and analogous structures, CCS structures would open a new field of research.

The calculations indicate that the conducting area is indeed restricted to the crystal channels that are occupied by the embedded Li atoms. Though there exist additional lateral conductive protrusions (dead tips) that point from one channel towards the neighboring Li wires, the latter are not capable of initiating any considerable charge equilibration with the neighboring tracks. On the one hand, the energy barriers between these protrusions and the neighboring channels are too high to allow for thermal Li ionic diffusion. On the other hand, voltage breakthrough from one Li wire to a neighboring one along these protrusions due to excessive electric field strength is also impossible. For that case, consider e.g., a typical electronic application where the potential difference of ~1 V will be applied at the upper two surface electrodes of ~5 μm distance, then the typical potential difference between two Li nanowires in the Nickel Phosphides will be in the order of 100 μV. At the same time, for a distance between the "dead tips" of about 2 Å and, assuming that the electric field for breakthrough would be as low as only 1 MV/cm, one would require a potential difference of about 20 mV between the two Li nanowires to obtain the field breakthrough, i.e. a voltage that is about 200 times larger than the available in the realistic application.

Further, one should consider the possibility of capacitive cross-talk between two neighboring Li wires in the case of high frequency applications. With an estimated capacity between two 100 nm long nanowires in the order of $\sim 10^{-17}$ F or so, a supposed number of 10^8 nanowires per sample crystal, and a typical inter-nanowire potential difference as estimated above (100 μV), the total cross-talk currents will be less than ~0.6 nA for 1 kHz, ~0.6 μA for 1 MHz and ~ 0.6 mA for 1 GHz. Assuming that the total currents along the individual Li nanowires are in the order of some μA, one can see that cross-talking will be negligible only below the MHz range. This means that this electronic crystal will exhibit the above-mentioned peculiar electronic properties only at low frequencies, whereas at higher frequencies it will just act like a conventional resistance.

The substrate favored here is a crystalline Si wafer as in the usual TEMPOS structures. This should facilitate the epitaxial $Ni_{12}P_5$ crystal growth. However, a problem may arise in this case as Li is known to diffuse very easily into Si, thus affecting adversely the electronic silicon properties and leading to an under-stoichiometric occupation of the channels in the $Ni_{12}P_5$ crystals by Li.

Therefore, one might have to think at depositing first a thin epitaxial barrier layer onto the Si that would impede the Li diffusion but still enable the epitaxial crystal growth and maintain the charge exchange between the Li nanowires and the Si substrate.

6.4 Conclusion

We have studied the electronic structure of $Ni_{12}P_5$ with Li atoms incorporated into crystal lattice channels. The obtained results have led to the conclusion that the creation of such a new electronic structure $Ni_{12}P_5$ + Li can be realized under the thermodynamic conditions of crystal growth. This structure consists of a set of parallel Li nanowires in the natural crystal channels of $Ni_{12}P$ and can be considered as the first representative of a new family of nanoelectronic structures with a multitude of parallel current paths. Such structures can be regarded as useful add-ons to traditional track electronics that have promising perspectives of applications.

Acknowledgements D. Fuks is thankful to B. Leshem, D. Kronenblum, and D. Vingurt for the help in computer calculations.

References

1. Fink D (2004) Ion- track manipulations, Ion-track applications. In: Fink D, Apel P.Yu, Iyer R. H.,(eds) Transport processes in ion irradiated polymers, vol 65, Springer series in materials science. Springer, Berlin/Heidelberg, pp 227–317
2. Berdinsky A, Alegaonkar P, Yoo J, Lee H, Jung J, Han J, Fink D, Chadderton L (2007) Growth of carbon nanotubes in etched ion tracks in silicon oxide on silicon. NANO Br Rep Rev 2:59–67
3. Fink D, Petrov A, Hoppe K, Fahrner W, Papaleo R (2003) Etched ion tracks in silicon oxide and silicon oxynitride as charge injection or extraction channels for novel electronic structures. Nucl Instrum Methods Phys Res Sect B 218:355–361
4. Fink D, Chadderton L (2005) Ion-solid interaction: status and perspectives. Braz J Phys 35(3b):0103–0133
5. Alfonta L, Fink D, Klinkovich I, Bukelman O, Kiv A, Fuks D (2008) Nuclear track membranes for biosensing and biocatalysis applications. P-71106-USP
6. Hoppe K, Fink D, Fahrner WR (2008) Metalized nuclear tracks in quasi MOS structures for nanoelectronic devices. J Electrochem Soc 155:7–11
7. Fink D (2004) Ion tracks in polymers. In: Fink D (ed) Fundamentals of ion irradiated polymers, vol 63, Springer series in materials science. Springer, Berlin/Heidelberg, pp 171–206
8. Fink D, Kiv A, Fuks D, Tabacnics M, de Rizutto AM, de Silva ODA, Chandra A, Golovanov V, Ivanovskaya M, Khirunenko L (2007) Irradiation-induced pulsations of reverse biased metal oxide/silicon structures. Appl Phys Lett 91:083512/1-3
9. Fink D, Kiv A, Golovanov V, Chen J, Chandra A, Ivanovskaya M, Khirunenko L, Fuks D (2008) Tin dioxide on semiconductor as material for new electronics. J Mater Sci Mater Electron 19:1222–1227

10. Fink D, Kiv A, Fuks D, Saad A, Vacik J, Hnatowicz V, Chandra A (2010) Conducting swift heavy ion track networks. Radiat Eff Defect Solid 165:227–244
11. Fink D, Cruz S, Munoz G, Kiv A (2011) Current spikes in polymeric latent and funnel-type ion tracks. Radiat Eff Defect Solid 166:373–388
12. Fink D, Chandra A, Saad A, Fahrner WR, Hoppe K, Alegaonkar P, Berdinsky A, Grasser D, Lorenz R (2008) Ion track-based electronic elements. Vacuum 82:900–905
13. Berdinsky AS, Fink D, Yoo JB, Chun HG, Chadderton LT, Petrov AV (2005) Conducting properties of planar irradiated and pristine silicon- fullerene – metal structures. Appl Phys A Mater Sci Proc 80:1711–1715
14. Fink D (2005) Novel ion track-based electronic structures – an overview. HMI/ISL-Information, Hahn-Meitner Institut Berlin, pp 2–5
15. Fink D, Chandra A, Opitz Coutureau J, Fahrner WR, Hoppe K, Papaleo RM (2007) Tunable electronically anisotropic materials with ion-irradiated polysilanes on semiconductor. Appl Phys A 86:469–476
16. Fink D, Vacik J, Hnatowicz V, Munoz GH, Alfonta L, Klinkovich I (2010) Funnel-type etched ion tracks in polymers. Radiat Eff Defect Solid 165:343–361
17. Siwy Z, Behrends J, Fertig N, Fulinski A, Martin CR, Neumann R, Trautmann C, Molares ET (2004) Nanovorrichtung für einen geladenen Teilchenfluss und Verfahren zu deren Herstellung. German patent DE 10244914A1
18. Fink D, Klinkovich I, Marks RS, Kiv A, Fuks D, Fahrner WR, Alfonta L (2009) Glucose determination using a re-usable enzyme-modified membrane sensor. Biosens Bioelectron 24:2702–2706
19. Alfonta L, Bukelman O, Chandra A, Fahrner WR, Fink D, Fuks D, Golovanov V, Hnatowicz V, Hoppe K, Kiv A, Klinkovich I, Landau M, Morante JR, Tkachenko NV, Vacík J, Valden M (2009) Strategies towards advanced ion track-based biosensors. Radiat Eff Defect Solid 164:431–437
20. Fink D, Kiv A, Fuks D, Munoz G, Cruz S, Fahrner W, Hoppe K (2011) Collective interaction in ion track electronics. Comput Model New Technol 15:7–18
21. Fink D, Munoz GH, Vacik J, Alfonta L (2011) Pulsed biosensing. IEEE Sens J 11(4):1084–1087
22. Hoppe K, Fahrner WR, Fink D, Dhamodoran S, Petrov A, Chandra A, Saad A, Faupel F, Chakravadhanula VSK, Zaporotchenko V (2003) An ion track based approach to nano- and micro-electronics. Nucl Instrum Method Phys Res B 218:355–361
23. Fowler HA, Erginsoy C (1967) Is proton channelling a diffraction process? Phys Lett A 27:390–391
24. Feldman LC, Mayer JW, Picraux STA (1982) Materials analysis by ion channelling: submicron crystallography. Academic Press, New York
25. Ryssel H, Ruge I (1986) Ion implantation. Wiley, New York
26. Deepak NK, Rajasekharan K, Neelakandan K (2000) Computer simulation of proton channeling in silicon. Pramana J Phys 54:845–856
27. Sloan J, Kirkland AI, Hutchison JL, Green MLH (2002) Chem Commun 13:1319–1332
28. Kirkland AI, Meyer RR, Sloan J, Hutchison JL (2005) Structure determination of atomically controlled crystal architectures grown within single wall carbon nanotubes. Microsc Microanal 11(5):401–409
29. Fuks D, Strutz A, Kiv A (2005) Bonding of Cr and V in FeAl B2 phase. Int J Quantum Chem 102:606–611
30. Fuks D, Strutz A, Kiv A (2006) Influence of alloying on the thermodynamic stability of FeAl B2 phase. Intermetallics 14:1245–1251
31. Fuks D, Zhukovskii YuF, Kotomin EA, Ellis DE (2006) Metal film growth on regular and defective MgO (001) surface: a comparative ab initio simulation and thermodynamic study. Surf Sci 600:L99–L104
32. Barzilai S, Argaman N, Froumin N, Fuks D, Frage N (2008) First-principles modelling of metal layer adsorption on CaF_2 (111). Surf Sci 602:1517–1524

33. Fuks D, Vingurt D, Landau M, Herskowitz M (2010) DFT study of sulfur adsorption at the (001) surface of metal-rich nickel phosphides: effect of Ni/P ratio. J Phys Chem C 14(31):13313–13321
34. Vingurt D, Fuks D (2010) Ab initio study of low-temperature phase transformations in ternary solid solution. Intermetallics 18:359–368
35. Fuks D, Shapiro D, Kiv A, Golovanov V, Liu CC (2011) Ab initio calculations of surface electronic states in Indium oxide. Int J Quantum Chem 111(9):1902–1906
36. Blaha P, Schwarz K, Madsen G, Kvasnicha D, Luitz J (2008) WIEN2k. Getreidemarkt 9/156 A-1060, Wien